A R C H I V E O F M E C H A N I C A L E N G I N E E R I N G

VOL. LXV 2018 Number 4

DOI: 10.24425/ame.2018.125439

Key words: geometrical nonlinearity, unsteady aerodynamics, bending mode, torsional mode, aeroelasticity, flexible structure

KAMRAN AHMAD[1], *ZHIGANG WU*[2], *HAMMAD RAHMAN*[1]

LIMIT CYCLE OSCILLATION PREDICTION BASED ON FINITE ELEMENT-MODAL APPROACH

The central theme of this work was to analyze high aspect ratio structure having structural nonlinearity in low subsonic flow and to model nonlinear stiffness by finite element-modal approach. Total stiffness of high aspect ratio wing can be decomposed to linear and nonlinear stiffnesses. Linear stiffness is modeled by its eigenvalues and eigenvectors, while nonlinear stiffness is calculated by the method of combined Finite Element-Modal approach. The nonlinear modal stiffness is calculated by defining nonlinear static load cases first. The nonlinear stiffness in the present work is modeled in two ways, i.e., based on bending modes only and based on bending and torsion modes both. Doublet lattice method (DLM) is used for dynamic analysis which accounts for the dependency of aerodynamic forces and moments on the frequency content of dynamic motion. Minimum state rational fraction approximation (RFA) of the aerodynamic influence coefficient (AIC) matrix is used to formulate full aeroelastic state-space time domain equation. Time domain dynamics analyses show that structure behavior becomes exponentially growing at speed above the flutter speed when linear stiffness is considered, however, Limit Cycle Oscillations (LCO) is observed when linear stiffness along with nonlinear stiffness, modeled by FE-Modal approach is considered. The amplitude of LCO increases with the increase in the speed. This method is based on cantilevered configuration. Nonlinear static tests are generated while wing root chord is fixed in all degrees of freedom and it needs modification if one requires considering full aircraft. It uses dedicated commercial finite element package in conjunction with commercial aeroelastic package making the method very attractive for quick nonlinear aeroelastic analysis. It is the extension of M.Y. Harmin and J.E. Cooper method in which they used the same equations of motion and modeled geometrical nonlinearity in bending modes only. In the current work, geometrical nonlinearities in bending and in torsion modes have been considered.

[1] *Institute of Space Technology, P.O. Box 2750 Islamabad, 44000, Pakistan.*
Email: nkamran128@yahoo.com

[2] *Beihang University of Aeronautics and Astronautics, China.*

Nomenclature

$\mathbb{M}$, $\mathbb{K}$, $\mathbb{F}$	structural physical mass/stiffness/force vectors
M, K, F	structural modal mass/stiffness/force vectors
X	physical displacement (bending and twist) vector
x	physical bending displacement vector
θ	physical twist displacement vector
θ_0	initial twist vector
q	modal displacement vector
A_r	nonlinear stiffness coefficients
AIC	aerodynamic influence matrix
A_n	Karpel's rational fraction approximation aerodynamic matrices
V, L, M	velocity, lift, pitching moment
N	number of DOF in FE model
NA	number of nonlinear stiffness coefficients
NR	number of DOF in reduced modal model
NT	number of nonlinear static test cases
A_w	lift curve slope
B	semi-chord
C	chord
k	reduced frequency
q	dynamic pressure
S	semi wing span
ρ	air density
Γ	circulation
m	number of aerodynamic lag terms
Φ	eigenvectors/mode shapes
A_0, A_1, A_2	Karpel's minimum state approximation matrices of order $NR \times NR$
D, E	rectangular Karpel's minimum state approximation matrices or order $NR \times m$ and $m \times NR$ respectively
$p = sL/V$	non dimensional complex Laplace

1. Introduction

Extensive work has been done on aeroelastic performance of high aspect ratio wings. Notably, Hodges and Patil [1–5] have used geometrically exact, fully intrinsic theory [6] to model structure and Peters and Johnson in-flow theory [7] to model aerodynamics and complete the aeroelastic formulation of high aspect ratio wing. In their work, they have shown to have drastic change in the structural and aeroelastic characteristics of high-aspect-ratio wings under nominal wing

loading. The type of nonlinear aeroelastic behavior is intimately connected with the distribution of modal frequencies relative to each other and the corresponding normal mode shapes including flap-wise bending, torsion and edgewise bending modes. Geometrical nonlinearities appear because of large tip deflection under normal flight condition. Aeroelastic behavior changes because of bending–torsion coupling and because of the changes in unsteady aerodynamic loading. Moreover, three dimensional effects of aerodynamics are quite small for the high-aspect ratio wings. The structural nonlinear effects were quite small for the steady state calculations. In pioneering work [8], high aspect ratio wing problem was studied. Using linear finite element analysis (FEA) and 2D unsteady strip theory aerodynamics, authors indicated that including flexible deformation modes has an obvious effect on predicted aircraft stability. Aeroelastic characteristics of highly flexible aircraft was investigated in [9]. The complete aircraft was modeled using 16 modes of vibration, including rigid-body modes. In [10] the authors theoretically and experimentally investigated flutter and limit cycle oscillations using a nonlinear beam model and ONERA stall model. Authors of [11] have presented nonlinear aeroelastic analysis using geometrically exact structural theory and a non-planar, fixed-wake aerodynamic theory. The results presented shed light on the importance of various types of geometrical nonlinearities on the aeroelastic behavior of high-aspect-ratio wings. There is negligible difference between the air-loads calculated using the correct non-planar wing geometry as compared to loads calculated assuming a planar wing. In further work [12] they have presented analysis with material anisotropy, geometrical nonlinearities of the structure, unsteady flow behavior, and dynamic stall. In [13] structural equations of motion based on nonlinear beam theory [14] along with original ONERA aerodynamic stall model [15] have been used to study the effects of geometric structural nonlinearity on flutter of high-aspect-ratio wings. Large static pre-flutter deformations in the vertical direction were considered. Other reserchers used a combined FE-Modal approach to handle nonlinear structural stiffness in aeroelastic problems [16]. The output from a series of static finite element test cases is transformed into modal coordinates using the mode shapes of the underlying linear system. Regression analysis is then performed in order to extract the nonlinear stiffness coefficients in the modal co-ordinate system. In the extension to their previous work, authors in [17] have used FE-Modal approach to model nonlinear stiffness and to predict limit cycle oscillation of high aspect ratio wing for un-deflected and deflected wing. How flutter speed is decreased in high aspect ratio wing with tip deflection has been demonstrated by Kamran et al [18]. In their further work [19], authors demonstrated Finite Element-Modal approach to predict tip deflection and tip twist using bending and torsional modes nonlinearities both.

The main contributions of the present work include:

1) development of the elastic beam and elastic shell model and to perform modal analysis using finite element method;
2) development of the nonlinear structure model using FE-Modal approach in bending only and in bending–torsion both;

3) identification of LCO in high aspect ratio wing structure using nonlinear structural stiffness.

2. Formulation

2.1. Finite Element-Modal approach

The equation of motion of dynamic system in physical coordinate system including geometrical nonlinearity is given as

$$[\mathbb{M}]\left\{\ddot{Y}\right\} + [\mathbb{C}]\left\{\dot{Y}\right\} + [\mathbb{K}_L]\{Y\} + \{\mathbb{K}_{NL}(Y)\} = \{\mathbb{F}\}. \tag{1}$$

Here, $\mathbb{M}$, $\mathbb{C}$ and $\mathbb{K}_L$ are the $2N \times 2N$ mass, damping and linear stiffness matrices, while $\mathbb{K}_{NL}$, $\mathbb{F}$ and $\mathbb{Y}$ are the $2N \times 1$ nonlinear stiffness, nodal applied force and spatial displacement vectors, respectively. The physical to modal coordinate transformation is given as

$$\{Y(x,\theta,t)\} = [\Phi(x,\theta)]\{q(t)\}, \tag{2}$$

where, $q(t)$ is the $NR \times 1$ vector of generalized modal coordinates. This vector is time dependent. $\Phi(x,\theta)$ is the $2N \times NR$ matrix. The number of degree of freedom in reduced order model (NR) is dependent on the frequency range of interest. However, NR is much less than N. Transforming the equation (1) into modal coordinates using equation (2) and pre-multiplying with Φ^T

$$\left[\Phi^T\right][\mathbb{M}][\Phi]\{\ddot{q}\} + \left[\Phi^T\right][\mathbb{C}][\Phi]\{\dot{q}\} + \left[\Phi^T\right][\mathbb{K}_L][\Phi]\{q\} + \\ + \left[\Phi^T\right]\{\mathbb{K}_{NL}(X)\}[\Phi]\{q\} = \left[\Phi^T\right]\{\mathbb{F}\}. \tag{3}$$

The advantage of transforming them into modal coordinates is that the system of equations becomes uncoupled because of orthogonality of the modes. Hence we get

$$[M]\{\ddot{q}\} + [C]\{\dot{q}\} + [K_L]\{q\} + \{K_{NL}(q)\} = \{F\}. \tag{4}$$

Here, M, C and K_L are the diagonal matrices of order $NR \times NR$. The order of modal coordinate vector $\boldsymbol{q}$, nonlinear modal stiffness vector $\boldsymbol{K}_{NL}$ and modal force vector $\boldsymbol{F}$ is $NR \times 1$. Nonlinear stiffness vector is the function of modal coordinate q.

2.2. Methodology for generating nonlinear static cases

The implementation of the finite element-modal approach is based on nodal deflections obtained from a number of prescribed static non-linear load cases. Thus, when a static system is considered and damping term ignored, the equations of motion, given by equation (4) reduces to

$$[K_L]\{q\} + \{K_{NL}(q)\} = \{F\}. \tag{5}$$

The total stiffness is considered to be composed of linear and nonlinear stiffness. Hence left-hand side may be considered as stiffness restoring force whiles the right-hand side in equation (5) is the statically applied load. If there exist a vector of static loads/moments and corresponding displacements/rotations, then there should exist stiffness matrix, relating the applied load to the corresponding displacements, whose coefficients need to be determined.

Two factors are important while generating nonlinear static load cases, the spatial distribution of the load over the structure and the magnitude of the load. Variation in the spatial distribution of a static case will result in a different level of modal inclusion. While magnitude of overall load would change the corresponding displacements and these displacements may or may not be in nonlinear region. Rearranging equation (5), one gets

$$\{F\} - [K_L]\{q\} = \{K_{NL}(q)\}\,. \tag{6}$$

It is assumed here that nonlinear cross coupling is important and hence load applied purely in the shape of one mode may induce a displacement response that is combination of more than one mode. Physical load/moment cases may be generated as the weighted sum of mode shapes and is given as

$$\{\mathbb{F}\} = \sum_{r=1}^{NR} a_r\{\Phi\}_r + a_r M, \tag{7}$$

here $\{\mathbb{F}\}$ is the total force applied on the structure which is the sum of bending load and twisting moment and it is $2N \times 1$, a_r is the scalar weighting factors and are selected so that the deflection is in the nonlinear region. Eigenvector matrix can be obtained from normal mode analysis by using any proprietary FE package. Its order is $2N \times NR$ containing vertical deflection and twist along the span axis. The transformation of nodal load/moment and displacement/rotation into the modal space can be calculated as

$$\{F\} = \left[\Phi^T\right]\{\mathbb{F}\} \;\Rightarrow\; \{q\} = \left(\left[\Phi^T\right][\Phi]\right)^{-1}\left[\Phi^T\right]\{Y\}. \tag{8}$$

2.3. Regression analysis

Upon completion of the static nonlinear test cases and with the acquired data of load/moment and displacement/rotation in modal space, the nonlinear restoring force for each of the test cases can now be fitted to find the unknown nonlinear modal stiffness coefficients in a least squares sense. An ordinary polynomial approach is selected here for curve fitting. Simultaneous coupling of two modes is considered. This coupling includes bending–bending and bending–torsion. Authors of [20] have shown that simultaneous couplings of more than two modes for the symmetric structure are very weak and can safely be omitted. The nonlinear restoring forces in matrix form for a certain mode 'r' is given as

$$\begin{Bmatrix} F_1 - K_{L(r)}q_1 \\ F_2 - K_{L(r)}q_2 \\ \vdots \\ F_{NT} - K_{L(r)}q_{NT}] \end{Bmatrix} = \begin{bmatrix} q^3_{1(1)} & q^3_{2(1)} & q^3_{3(1)} & \cdots \\ q^3_{1(2)} & q^3_{2(2)} & q^3_{3(3)} & \cdots \\ \vdots & \vdots & \vdots & \vdots \\ q^3_{1(NT)} & q^3_{2(NT)} & q^3_{3(NT)} & \cdots \end{bmatrix} \begin{Bmatrix} A_1 \\ A_2 \\ \vdots \\ A_{NA} \end{Bmatrix}$$

$$\Rightarrow \{F_r\}_{NL} = [D_r]\{A_r\}, \tag{9}$$

here, $\{\boldsymbol{F_r}\}_{NL}$ is a $NT \times 1$ vector of nonlinear modal stiffness restoring forces, $[D_r]$ is $NT \times NA$ design matrix and $\{\boldsymbol{A_r}\}$ is $NA \times 1$ vector having the unknown values of nonlinear stiffness coefficients. Each row in matrix $[\boldsymbol{D}]$ refers to an evaluation using one of the NT data sets available. The subscripts in the bracket refer to the test load case that the data value originated from. NT should be greater than NR for exact solution.

2.4. Backward elimination of redundant terms

When all possible terms have been included in the design matrix $[\boldsymbol{D}]$, there is a possibility that matrix becomes singular or near to singular. Hence equation (9) becomes ill conditioned and cannot be solved directly. Singular value decomposition (SVD) is one of the methods to solve such ill conditioned problem. SVD allows writing an ill conditioned matrix in the form of three matrices which are given as

$$[D_r] = [U]\,[W]\,[V]^T, \tag{10}$$

here, $[\boldsymbol{U}]$ is an $NT \times NA$ and $[\boldsymbol{V}]$ is $NA \times NA$ matrix, and both are orthogonal. $[\boldsymbol{W}]$ is $NA \times NA$ diagonal matrix and all the diagonal elements are positive. It is important to note here that some of the elements in $[\boldsymbol{W}]$ may be zero in case it is singular or near to zero in case of near to singular matrix. Therefore, noncontributing elements are removed such that

$$[W]^{-1} = \begin{cases} \dfrac{1}{\sigma_i} & \text{if } \sigma_i > \text{tolerance}, \\ 0 & \text{otherwise}. \end{cases} \tag{11}$$

Nonlinear stiffness coefficients can be found by solving equation given as

$$\{A_r\} = [V]\,[W]^{-1}[U]^T\,\{F_r\}_{NL}\ . \tag{12}$$

To solve equation (12), the $[\boldsymbol{U}]$ and $[\boldsymbol{V}]$ matrices are also modified depending upon the number of columns removed from $[\boldsymbol{W}]$. Backward elimination methodology is used to remove terms which are less significant to the overall solution. Root mean square method may be used to find the contribution of each polynomial term and is given as

$$H(i,j) = \sqrt{\frac{1}{NT}\sum_{i=1}^{NT}\left(D_r(i,j)\,A_r(j)\right)^2}. \tag{13}$$

Situation would be ideal if all terms in the design matrix are used, however numerical solution may become unstable. Therefore, a pre-selected threshold value is chosen. Say, a particular term is eliminated if its contribution is less than 1%. Total contribution of retained terms should be near to 100%. During the backward elimination process, if all terms are exhausted, then the model in question is certainly a linear system and non non-linear stiffness terms are required. On the other hand, if this procedure stops at the first iteration, the numbers of polynomial terms considered are not sufficient to model restoring force and more terms should be added.

Significant terms for a particular non-linear modal restoring force once identified, the entire process is repeated for the next mode until the entire multi-mode model has been identified. The inertial and damping terms can be added to complete the governing equation in modal form.

2.5. Structural model verification

Verification process starts by performing linear and nonlinear static analyses through a commercial FEM code by applying a set of wing tip forces at the quarter chord and noting the tip deflection and twist at the three quarter chord. In vortex lattice method, vortices are places at the quarter chord and zero normal flow boundary condition is achieved at the control points, which is midway span-wise and at three quarter chord chord-wise. This constraint ensures that Kutta condition is met [21]. Using the nonlinear stiffness calculated through equation (9), and using same set of wing tip forces, FE-modal approach was used to calculate tip deflection and tip twist. Results have been plotted in Fig. 1 and Fig. 2 Wing tip deflection

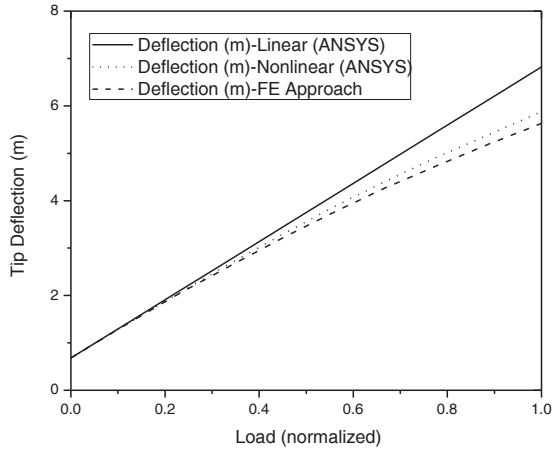

Fig. 1. Wing tip force vs. tip deflection comparison

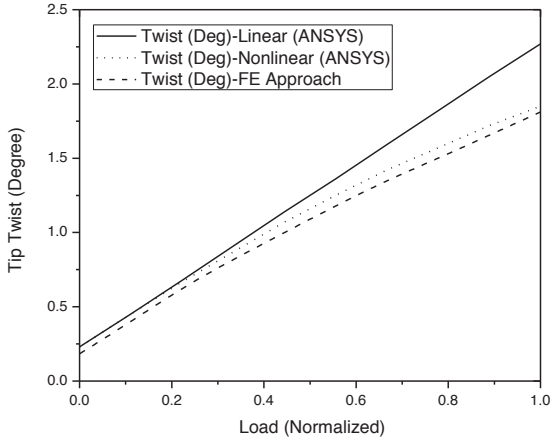

Fig. 2. Wing tip force vs. tip twist comparison

and wing tip twist calculated through FE-modal approach agrees well with the nonlinear results of FEM commercial code. This verifies that nonlinear stiffness calculated through equation (9) is valid and may be used for further analysis.

2.6. Linear aerodynamic model and Karpel's minimum state approximation

A good description of panel method has been given in [21] and [22]. Lift in this method is computed by the following equation

$$L = \rho V S \Gamma = \frac{\rho V^2}{2}[AIC]\{\theta + \theta_0\}, \tag{14}$$

where AIC is aerodynamic influence coefficient matrix. Each term of AIC (that is AIC_{ij}) relates the lift on each panel to the aerodynamics and angle of incidence of each element and also the aerodynamic pressure converting the equation (14) into modal coordinates, so one gets

$$L = \frac{\rho V^2}{2} AIC_R h + i\omega \frac{\rho V}{2} \frac{b}{k} AIC_I h = \frac{\rho V^2}{2}[Q]\{q + q_0\}. \tag{15}$$

Here, $[\boldsymbol{Q}]$ is generalized aerodynamics force matrix. Each term in $[Q]$ matrix has real part and imaginary part. Unsteady aerodynamic effects can be included by allowing the aerodynamic influence coefficient matrix to become complex function of reduced frequency and is given as

$$k = \frac{wb}{V}. \tag{16}$$

Harmonic motion of the lifting surface is assumed while deriving the equation (15). Karpel's minimum state approximation [23] for Q is given by the following the equation

$$[Q(p)] = A_0 + A_1 p + A_2 p^2 + D[pI - R]^{-1} Ep. \tag{17}$$

Here, A_0, A_1 and A_2 are $NR \times NR$ matrices, R is the diagonal matrix containing m lag term coefficients, D and E are rectangular matrices of $NR \times m$ and $m \times NR$ respectively, p the non-dimensional complex Laplace variable. The minimum state problem for a given R is nonlinear. It is solved iteratively by starting with an initial guess of D in which at least one term in each row and each column is nonzero. For a given D, A_0, A_1 and A_2 and E are calculated. The calculated E is then used to update A_0, A_1, A_2 and D. The entire sequence of least-square solutions forms a $D \rightarrow E \rightarrow D$ iteration which is repeated until the specified maximum number of iterations is reached. Combining equation (15) and equation (17) gives state space equations in which unsteady lift force is approximated using Karpel's minimum state approximation.

2.7. Computational aeroelastic model

Combining equations (4), (15) and (17) and writing the equations of motion in augmented state we get

$$\left[\overline{M}\right]\{\ddot{q}\} + \left[\overline{C}\right]\{\dot{q}\} + \left[\overline{K}_L\right]\{q\} + \{K_{NL}(q)\} = \frac{1}{2}\rho V^2 [D]\{x_a\}, \tag{18}$$

where x_a is a vector due to aerodynamic lag terms and $\left[\overline{M}\right]$, $\left[\overline{C}\right]$ and $\left[\overline{K}_L\right]$ are defined as

$$\begin{aligned} \left[\overline{M}\right] &= [M] - \frac{1}{2}\rho b^2 [A_2], \\ \left[\overline{C}\right] &= [C] - \frac{1}{2}\rho b V [A_1], \\ \left[\overline{K}_L\right] &= [K_L] - \frac{1}{2}\rho V^2 [A_0]. \end{aligned} \tag{19}$$

Equation (18) can be written in state space form as

$$\begin{Bmatrix} \ddot{q} \\ \dot{q} \\ \dot{x}_a \end{Bmatrix} = \begin{bmatrix} -\left[\overline{M}\right]^{-1}\left[\overline{C}\right] & -\left[\overline{M}\right]^{-1}\left[\overline{K}\right] & 0.5\rho V^2 [D]\left[\overline{M}\right] \\ I & 0 & 0 \\ E & 0 & \dfrac{V}{b}[R] \end{bmatrix} \begin{Bmatrix} \dot{q} \\ q \\ x_a \end{Bmatrix} - \begin{bmatrix} \left[\overline{M}\right]^{-1}\{K_{NL}(q)\} \\ 0 \\ 0 \end{bmatrix}, \tag{20}$$

$$Y = \begin{Bmatrix} \dot{q} \\ q \\ x_a \end{Bmatrix} \Rightarrow \dot{Y} = \begin{Bmatrix} \ddot{q} \\ \dot{q} \\ \dot{x}_a \end{Bmatrix}, \tag{21}$$

$$\overline{A} = \begin{bmatrix} -\left[\overline{M}\right]^{-1}\left[\overline{C}\right] & -\left[\overline{M}\right]^{-1}\left[\overline{K}\right] & 0.5\rho V^2[D]\left[\overline{M}\right] \\ I & 0 & 0 \\ E & 0 & \dfrac{V}{b}[R] \end{bmatrix}. \tag{22}$$

The final form of equation is given as

$$\dot{Y} = \overline{A}Y - \begin{Bmatrix} \left[\overline{M}\right]^{-1}\{K_{NL}(q)\} \\ 0 \\ 0 \end{Bmatrix}. \tag{23}$$

Methodology of FE-Modal approach presented in [16, 17, 23] and [24] has been used here to model geometrical nonlinearity in this work. Nonlinearity has been modeled in bending as well in torsion modes and hence this work is the extension of [16, 17] in which only bending nonlinearity was considered and torsion was taken as linear. Bending modes cross coupling is considered. Bending–bending and bending–torsion cross coupling has been considered in this work. 4^{th} order Runge Kutta method is used to solve equation (23).

3. Computational model

A high aspect ratio straight wing [1] is analyzed. Its structural properties are given in Table 1. Finite element wing model and its first five mode shapes are shown in Fig. 3. For the cantilever shell model, the first, second and fifth are

Table 1.

Wing tip force vs. tip deflection comparison

S. No	Structural characteristics	Value
1	Half span	16 m
2	Chord	1 m
3	Mass per unit length	0.75 kg/m
4	Moment of inertia (50% chord)	0.1 kgm
5	Spanwise elastic axis	50% chord
6	Center of gravity	50% chord
7	Bending rigidity	2×10^4 Nm^2
8	Torsional rigidity	1×10^4 Nm^2
9	Edge wise bending rigidity	5×10^6 Nm^2
Flight condition		
1	Altitude	20 km
2	Air density	0.0889 kg/m^3
3	Lift curve slope	5.58

bending modes, while the third and fourth are torsion and flap-wise bending modes. The higher modes are difficult to excite and are expected to have few effects on the dynamic analysis. It is important to mention that these frequencies values are for straight wing configuration. However, there is variation in torsion and flap-wise

Finite element wing model

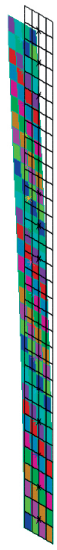

0.35 Hz (1st bending)

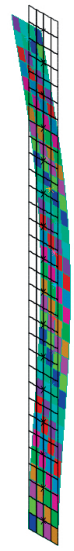

2.24 Hz (2nd bending)

5.02 Hz (1st torsion)

5.72 Hz (1st in-plane bending)

6.31 Hz (3rd bending)

Fig. 3. Wing tip force vs. tip deflection comparison

bending frequencies when wing is deflected. This variation is shown in Fig. 2. This implies that the dynamic behavior of the straight undeflected wing would be different from that of deflected wing. However, analysis presented in this work is for the straight undeflected wing model. It is obvious from Fig. 4 that nonlinear behavior is distinct when vertical deflection is more than 2.5 m for the particular structure considered. Therefore, in order to model geometrical nonlinearity, forces are selected in such a way that the corresponding displacements should be more than 2.5 m for the considered configuration. For a realistic upper bound for vertical deflection could be 6 m. Similarly, nonlinear stiffness in torsion becomes obvious when flexible twist is more than 1°. Hence, moments values should be selected such that twist value should be greater than this threshold value.

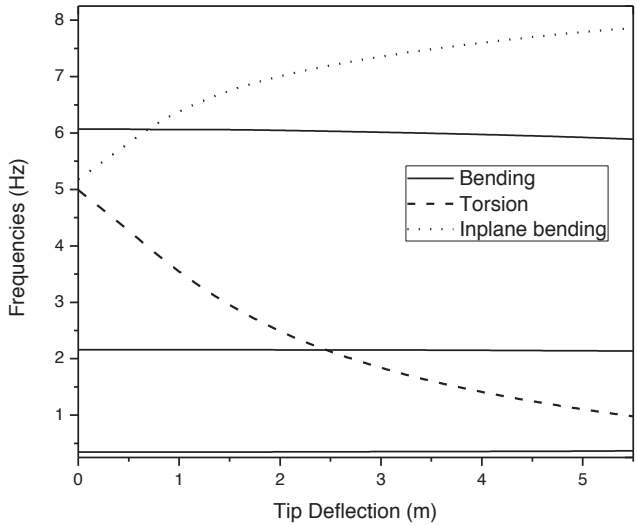

Fig. 4. Frequencies variation vs. wing tip deflection

4. Results and discussion

Small initial deflection was given at the tip to initiate the disturbance. Tip twist time history below the flutter is shown in Fig. 5, while linear stiffness is considered. However, diverging response is obtained above flutter speed for linear structural system and is shown in Fig. 6. In the next step, nonlinear stiffness, calculated from the FE-modal approach is taken in calculation and the time history below the flutter speed is decaying as shown in Fig. 7. It is the same response as was the case with linear stiffness. However, a limit cycle oscillation is obtained above flutter speed as shown in Fig. 8. This was not the case when linear stiffness was considered. Hence nonlinear stiffness contains the vibration to a certain level. However, the amplitude of vibration increases with the speed above flutter speed

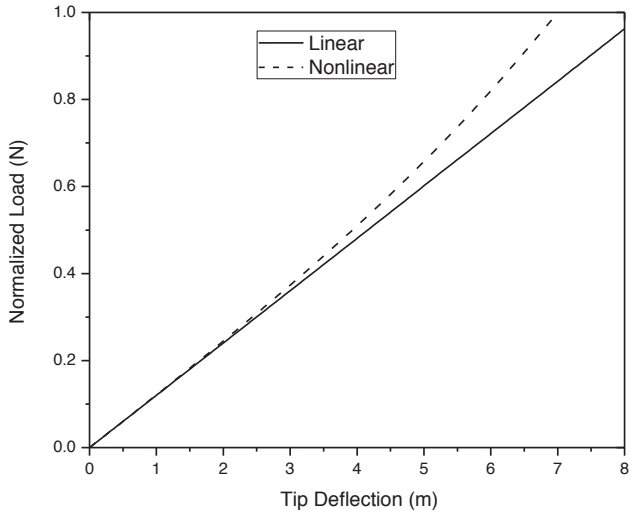

Fig. 5. Linear and nonlinear wing tip deflection of high aspect ratio wing

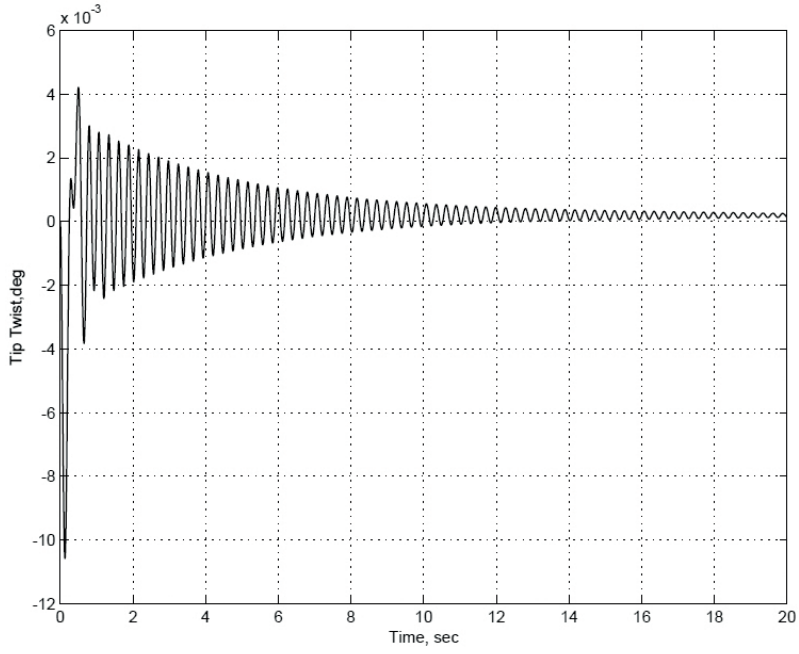

Fig. 6. Decaying behavior of Patil wing before flutter speed with linear stiffness

as shown in Fig. 9. Limit cycle oscillation is typical characteristic of nonlinear system. If the initial disturbance is sufficiently small, a stable LCO is expected above flutter speed. However, LCO may also arise below the flutter speed if the initial disturbance is sufficiently large. Majority of researchers attributed LCO to

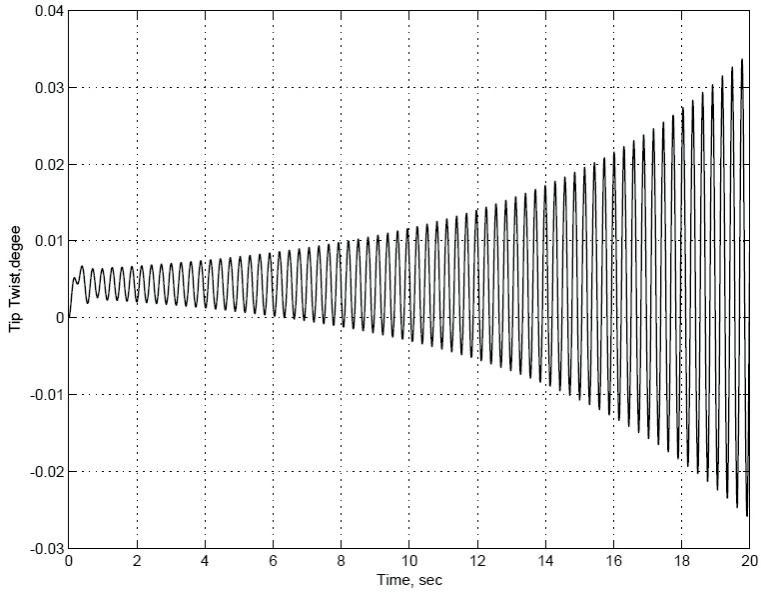

Fig. 7. Diverging behavior of Patil wing after flutter speed with linear stiffness

nonlinear aerodynamics. This nonlinear aerodynamics could be because of shocks wave motion or stall. However, damping, free play or structural nonlinearity may also lead to initiation of LCO.

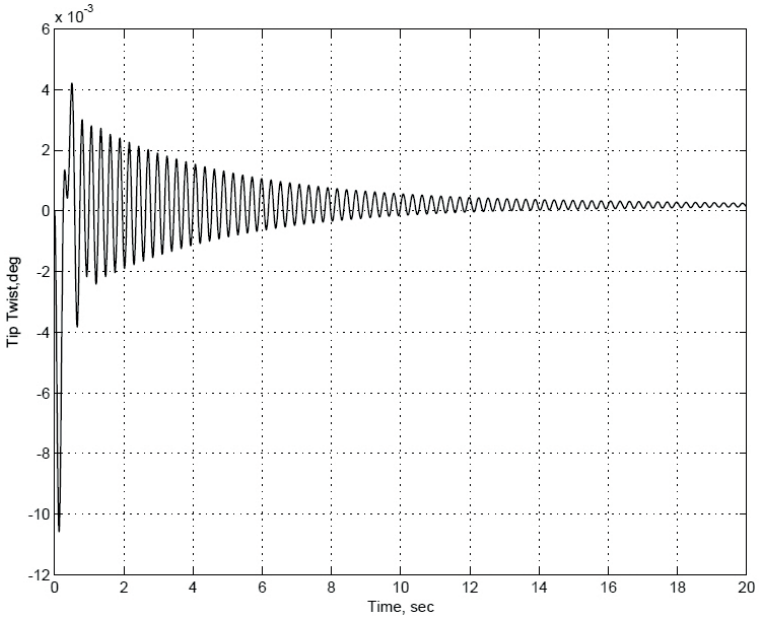

Fig. 8. Converging behavior of Patil wing before flutter speed with nonlinear stiffness

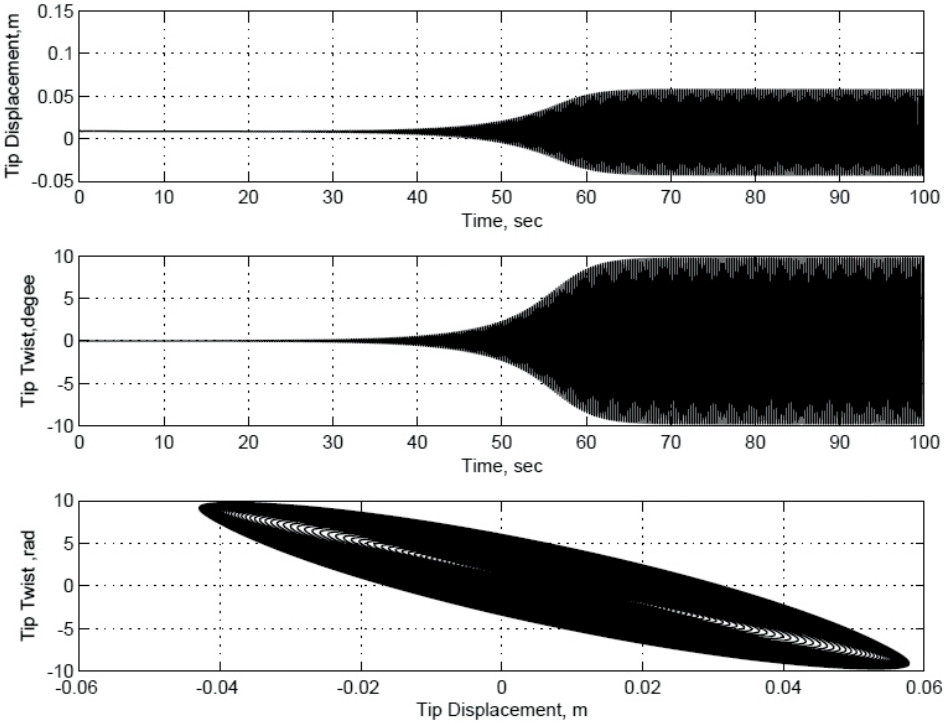

Fig. 9. Limit cycle oscillation of Patil wing above flutter speed

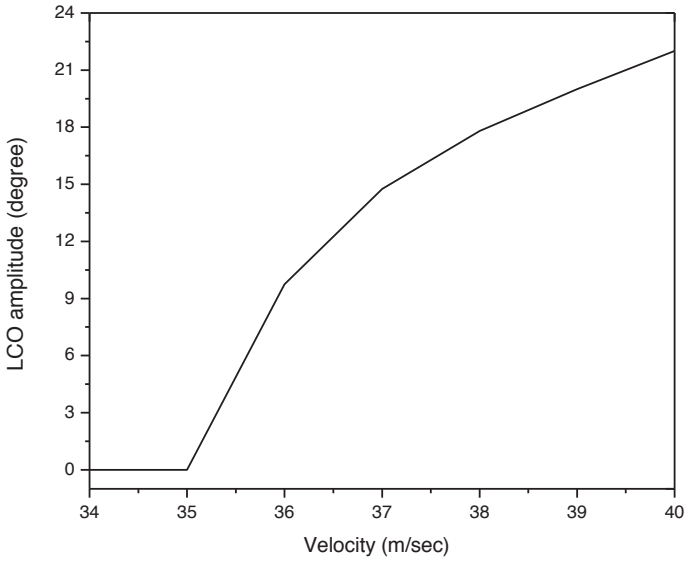

Fig. 10. Limit cycle oscillation twist amplitude vs. velocity

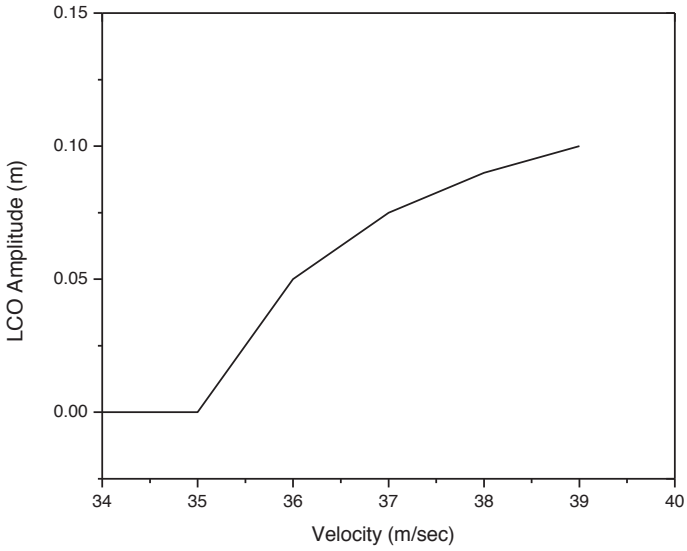

Fig. 11. Limit cycle oscillation bending amplitude vs. velocity

5. Conclusions

In this work, the geometrical nonlinearity encountered in High Altitude Long Endurance (HALE) aircraft wing is numerically investigated in time domain. Nonlinear structure is modeled by FE-Modal approach and aerodynamics forces are calculated by the generalized aerodynamic force from ZAERO package and Karpel's rational fraction approximation for linear unsteady aerodynamics prediction. Linear structure was simulated by eigenvalues and eigenvectors, while nonlinear structure was simulated by FE-Modal approach. High aspect ratio wing aeroelastically analyzed in cantilevered configuration. Commercial FEM package ANSYS is used for free vibration analysis and to get the natural frequencies along with mode shapes to be ultimately used in aeroelastic analysis. Equations of motion are solved using state-space model in modal coordinates. The time histories of the generalized modal coordinates show that at speed below the flutter speed, wing tip deformations experience decaying oscillation and finally approach steady state. Non-decaying motion is observed at the critical speed. At the flutter speed, all modes are responding at the same frequency value. Moreover, wing tip oscillations are increasing when linear stiffness is considered above flutter speed, an LCO is observed when nonlinear stiffness is also added. LCO is a typical characteristic of nonlinear system. It is the geometrical nonlinearity which is responsible for this LCO. A stable LCO is expected above flutter speed when the initial disturbance is sufficiently small. However, LCO may also arise below the flutter speed if the initial disturbance is sufficiently large. In stable LCO the motion returns the same LCO at larger time

while unstable LCO are those for which any disturbance causes the motion to move away from the unstable LCO and moves towards a stable LCO. From the study, it is evident that LCO could be identified with bending nonlinearity only; however, the amplitude in twist may/may not be correct. Moreover, bending nonlinearity is more important than torsional nonlinearity. No LCO is obtained when bending modes are kept linear and using torsional nonlinearity only.

6. Future work

Work will certainly be extended to, but not limited to the following topics:

1. Gust response.
2. Employing nonlinear structural models for full span configuration.
3. Incorporation of stall model.
4. Inclusion of rigid body modes.

Manuscript received by Editorial Board, March 17, 2018;
final version, September 10, 2018.

References

[1] M.J. Patil, D.H. Hodges, and C.E.S. Cesnik. Characterizing the effects of geometrical nonlinearities on aeroelastic behavior of high-aspect-ratio wings. In *Proceedings of the International Forum on Aeroelasticity and Structural Dynamics*, pages 501–510, Williamsburg, Virginia, USA, 22–25 June, 1999.

[2] M. Patil, D. Hodges, and C.E.S. Cesnik. Nonlinear aeroelastic analysis of aircraft with high-aspect-ratio wings. In: *Proceedings of the 39th Structures, Structural Dynamics, and Materials Conference*, pages 2056–2068, Long Beach, California, 20–23 April, 1998. doi: 10.2514/6.1998-1955.

[3] M.J. Patil, D.H. Hodges, and C.E.S. Cesnik. Nonlinear aeroelastic analysis of complete aircraft in subsonic flow. *Journal of Aircraft*, 37(5):753–760, 2000. doi: 10.2514/2.2685.

[4] M.J. Patil and D.H. Hodges. Flight dynamics of highly flexible flying wings. *Journal of Aircraft*, 43(6):1790–1799, 2006. doi: 10.2514/1.17640.

[5] M.J. Patil, D.H. Hodges, and C.E.S. Cesnik. Limit-cycle oscillations in high-aspect-ratio wings. *Journal of Fluids and Structures*, 15(1):107–132, 2001. doi: 10.1006/jfls.2000.0329.

[6] D.H. Hodges. A mixed variational formulation based on exact intrinsic equations for dynamics of moving beams. *International Journal of Solids and Structures*, 26(11):1253–1273, 1990. doi: 10.1016/0020-7683(90)90060-9.

[7] D.A. Peters and M.J. Johnson. Finite-state airloads for deformable airfoils on fixed and rotating wings. In *Proceedings of ASME Winter Annual Meeting: Aeroelasticity and Fluid/ Structure Interaction*, pages 1–28, New York, 6–11 Nov., 1994.

[8] M.C. van Schoor and A.H. von Flotow. Aeroelastic characteristics of a highly flexible aircraft. *Journal of Aircraft*, 27(10):901–908, 1990. doi: 10.2514/3.45955.

[9] C. Pendaries. From the HALE gnopter to the ornithopter – or how to take advantage of aircraft flexibility. In: *Proceedings of the 21st Congress of the International Council of the Aeronautical Sciences, Melbourne, Australia*, 13–18 Sept. 1998. Paper no. A98-31715.

[10] D. Tang and E.H. Dowell. Experimental and theoretical study on aeroelastic response of high-aspect-ratio wings. *AIAA Journal*, 39(8):1430–1441, 2001. doi: 10.2514/2.1484.

[11] M.J. Patil and D.H. Hodges. On the importance of aerodynamic and structural geometrical nonlinearities in aeroelastic behavior of high-aspect-ratio wings. *Journal of Fluids and Structures*, 19(7):905–915, 2004. doi: 10.1016/j.jfluidstructs.2004.04.012.

[12] M.J. Patil, D.H. Hodges, and C.E.S. Cesnik. Nonlinear aeroelasticity and flight dynamics of high-altitude long-endurance aircraft. *Journal of Aircraft*, 38(1):88–94, 2001. doi: 10.2514/2.2738.

[13] D.M. Tang and E.H. Dowell. Effects of geometric structural nonlinearity on flutter and limit cycle oscillations of high-aspect-ratio wings. *Journal of Fluids and Structures*, 19(3):291–306, 2004. doi: 10.1016/j.jfluidstructs.2003.10.007.

[14] D.H. Hodges and E.H. Dowell. Nonlinear equations of motions for the elastic bending and torsion of the twisted non-uniform rotor blades. Technical Report NASA-TN D-7818, 1974.

[15] C.T. Tran and D. Petot. Semi-empirical model for the dynamic stall of airfoils in view of the application to the calculation of response of a helicopter blade in forward flight. *Vertica*, 5(1):35–53, 1981.

[16] M.Y. Harmin and J.E. Cooper. Efficient prediction of aeroelastic behaviour including geometric non-linearities. In: *Proceedings of the 51st AIAA/ASME/ASCE/AHS/ASC Structures, Structural Dynamics, and Materials Conference*, paper no. 2010–2631, Orlando, Florida, USA, 12–15 April, 2010. doi: 10.2514/6.2010-2631.

[17] M.Y. Harmin and J.E. Cooper. Aeroelastic behaviour of a wing including geometric nonlinearities. *The Aeronautical Journal*, 115(1174):767–777, 2011. doi: 10.1017/S0001924000006515.

[18] K. Ahmad, Shigang Wu, and H. Rahman. Aeroelastic analysis of high aspect ratio wing in subsonic flow. In *Proceedings of 2013 10th International Bhurban Conference on Applied Sciences and Technology (IBCAST)*, pages 219–223, Islamabad, Pakistan, 15–19 Jan., 2013. doi: 10.1109/IBCAST.2013.6512157.

[19] K. Ahmad, H. Rahman, and H.J. Hasham. Nonlinear static aeroelastic analysis of high aspect ratio wing. In *Proceedings of 2014 11th International Bhurban Conference on Applied Sciences and Technology (IBCAST)*, pages 349–353, Islamabad, Pakistan, 14–18 Jan., 2014. doi: 10.1109/IBCAST.2014.6778168.

[20] M.I. McEwan, J.R. Wright, J.E. Cooper, and A.Y.T. Leung. A combined modal/finite element analysis technique for the dynamic response of a non-linear beam to harmonic excitation. *Journal of Sound and Vibration*, 243(4):601–624, 2001. doi: 10.1006/jsvi.2000.3434.

[21] J. Katz and A. Plotkin, *Low-Speed Aerodynamics*. 2nd edition, Cambridge University Press, 2001.

[22] J.R. Wright and J.E. Cooper. *Introduction to Aircraft Aeroelasticity and Loads*. 2nd edition, John Wiley & Sons, Ltd, 2015.

[23] M. Karpel. Design for active flutter suppression and gust alleviation using state-space aeroelastic modeling. *Journal of Aircraft*, 19(3):221–227, 1982. doi: 10.2514/3.57379.

[24] A.A. Muravyov and S.A. Rizzi. Determination of nonlinear stiffness with application to random vibration of geometrically nonlinear structures. *Computers & Structures*, 81(15):1513–1523, 2003. doi: 10.1016/S0045-7949(03)00145-7.